Wake attenuation in large Reynolds number dispersed two-phase flows

Frederic Risso, Véronique Roig, Zouhir Amoura, Guillaume Riboux, Anne-Marie Billet

Wake attenuation in large Reynolds number dispersed two-phase flows

By Frédéric Risso[1,*], Véronique Roig[1], Zouhir Amoura[1], Guillaume Riboux[1] and Anne-Marie Billet[2]

[1]*Institut de Mécanique des Fluides, UMR 5502 CNRS/INP/UPS Allée Camille Soula, 31400 Toulouse, France*
[2]*Laboratoire de Génie Chimique, UMR 5503 CNRS/INP/UPS, 5 rue Paulin Talabot, BP1301, 31106 Toulouse Cedex 1, France*

The dynamics of high Reynolds number-dispersed two-phase flow strongly depends on the wakes generated behind the moving bodies that constitute the dispersed phase. The length of these wakes is considerably reduced compared with those developing behind isolated bodies. In this paper, this wake attenuation is studied from several complementary experimental investigations with the aim of determining how it depends on the body Reynolds number and the volume fraction α. It is first shown that the wakes inside a homogeneous swarm of rising bubbles decay exponentially with a characteristic length that scales as the ratio of the bubble diameter d to the drag coefficient C_{d}, and surprisingly does not depend on α for $10^{-2} \leq \alpha \leq 10^{-1}$. The attenuation of the wakes in a fixed array of spheres randomly distributed in space ($\alpha = 2 \times 10^{-2}$) is observed to be stronger than that of the wake of an isolated sphere in a turbulent incident flow, but similar to that of bubbles within a homogeneous swarm. It thus appears that the wakes in dispersed two-phase flows are controlled by multi-body interactions, which cause a much faster decay than turbulent fluctuations having the same energy and integral length scale. Decomposition of velocity fluctuations into a contribution related to temporal variations and that associated to the random character of the body positions is proposed as a perspective for studying the mechanisms responsible for multi-body interactions.

Keywords: wake; dispersed flow; bubbles; solid spheres; random network; multi-body interactions

1. Introduction

Dispersed two-phase flows consist of a population of bodies (solid particles, drops or bubbles) immersed in a fluid. These are often encountered in nature (rains, breaking waves) and in industrial applications, such as oil transport (pipelines), energy production (vapour generators, heat exchangers) and chemical engineering (bubble columns, chemical reactors). Their dynamics are controlled by complex interactions between continuous and dispersed phases. In particular, a crucial phenomenon is the flow generation by the motions of the bodies relative to the

* Author for correspondence (frederic.risso@imft.fr).

continuous phase. Let us consider the simplest situation in which bodies of size d move at velocity V in a fluid otherwise at rest. In the limit of vanishing volume fraction of the dispersed phase α, we may expect that body interactions are negligible so that the flow generated by a single body is relevant to describe the perturbation generated in the continuous phase. This flow depends on the Reynolds number $Re = Vd/\nu$. In the Stokes regime ($Re = 0$), the flow perturbation decays as r^{-1}, r being the distance to the body. Owing to this slow decay, the simple addition of the flows induced by randomly distributed bodies leads to the divergence of the velocity variance with the size of the container (Calfish & Luke 1985). At finite Reynolds numbers, a wake develops behind the body, which decays with the downstream distance z as z^{-1} in the laminar case and $z^{-2/3}$ in the turbulent one, leading again to the divergence of the velocity variance (Parthasarathy & Faeth 1990; Koch 1993). Even if the divergence problem exists whatever the Reynolds number is, the mechanisms that lead to finite velocity variance in real situations certainly depend on the Reynolds number.

Some mechanisms have been proposed to prevent the divergence due to the slow decay of the wake. Parthasarathy & Faeth (1990) investigated solid particles falling at a very low concentration $\alpha < 10^{-4}$, for $38 < Re < 800$. They reproduced the experimental variance from the summation of the flows generated by isolated bodies by considering that the wake vanishes for $z > L = 175d$, where it could not maintain its coherence in the ambient fluctuations generated by the other bodies. This approach may be valid only when the average distance between the bodies $l_b = (\pi/6\alpha)^{1/3} d$ is large enough so that interactions occur in a region where the wake intensity is sufficiently small and does not contribute significantly to the velocity variance. Since l_b is already close to $4d$ at $\alpha = 10^{-2}$, interactions have to be considered in most of the practical situations.

Koch (1993) proposed a theory for the velocity fluctuations in a sedimenting suspension where particles have Oseen's wakes. For $1 < Re < 10$, the velocity fluctuations are controlled by a screening mechanism due to a deficit of particles in the wake of a test particle. As a consequence, the velocity disturbance in the wake was found to be screened for $z > L = O(d\alpha^{-1})$. Experimental evidence of wake attenuations was found by Cartellier & Rivière (2001) in uniform bubbly flows for $Re = O(10)$. This attenuation was shown to be related to a deficit of bubbles in the near wake up to a distance that evolved roughly as $\alpha^{-0.3}$.

A non-uniform spatial distribution of the bodies is however not the only mechanism that can lead to wake attenuation. Hunt & Eames (2002) investigated theoretically the effect exerted on a wake by a large-scale external strain. In particular, the effects of a sequence of positive and negative strains, which can be observed in complex flow, cause diffusion and cancellation of vorticity and consequently an attenuation of the wake defect. Another mechanism is the intermingling between the wakes generated by neighbour bodies—by mixing vorticity components of opposite sign, interacting wakes can make themselves disappear rapidly. White & Nepf (2003) and Eames *et al.* (2004) have modelled this mechanism for a random array of bodies in a uniform flow. The conditionally averaged velocity field around a test body is governed by a momentum equation with a distributed sink term associated with the drag forces exerted by the other particles. This results in the exponential extra

attenuation $\exp(-z/L)$ of the velocity defect behind the test body compared with an isolated body. The attenuation length L scales as the ratio of the size of the body to its drag coefficient C_{d}, and as the reciprocal of the volume fraction; for an array of spheres, it can be written as $L=2d/3\alpha C_{\mathrm{d}}$.

The dynamics of dispersed two-phase flows at non-zero Reynolds numbers therefore depends on the modification of individual wakes due to multi-body interactions. Experimental investigations of wakes behind bodies belonging to a dispersed phase are required to discriminate between the possible mechanisms that may cause wake attenuation. In particular, it would be useful to determine how the attenuation length L evolves with the body Reynolds number and the volume fraction. This paper presents some results of various experimental investigations at the large Reynolds number ($100<Re<1000$) of complementary situations involving either bubbles or rigid spheres, fixed or moving bodies, isotropic turbulence or wake-induced agitation. In §2, the flow field induced by a test bubble within a homogeneous rising swarm of bubbles is compared with that induced by an isolated rising bubble. Quantitative measurements of the attenuation length in bubbly flows are provided and discussed in §3. Then, the evolution of the wake of a rigid sphere in an ambient turbulent flow is investigated in §4 and compared with that of a sphere in a random array of identical spheres in §5. Finally, new perspectives concerning wake interactions are discussed in §6.

2. Liquid flow induced by rising bubbles

Before discussing the attenuation of wakes due to multi-body interactions, it is useful to describe the flow generated by a single body. Ellingsen & Risso (2001) investigated the case of a bubble of a 2.5 mm equivalent diameter rising in water at a velocity $V=309\ \mathrm{mm\ s^{-1}}$. The flow regime was dominated by inertia with large Reynolds and Weber numbers: $Re=8\times10^2$ and $We=\rho V^2 d/\sigma=3.6$ (ρ being the density and σ the surface tension of water). The rising bubble approximately adopted a constant spheroidal shape with an aspect ratio of two and performed path oscillations. Combining laser Doppler anemometry (LDA) and high-speed imaging (HSI), the maximal velocity perturbation induced in the liquid was determined as a function of the vertical distance z to the bubble. The thin line in figure 1*a* shows the vertical perturbation—in front of the bubble ($z<0$) the flow is potential and a long wake develops behind (still 5% of V at $z=70d$). The flow in the wake includes two contributions due to a quasi-steady wake that spreads around the bubble trajectory and wake vortices generated at the rear. However, the latter contribution is only significant close to the bubble and the wake decay is predicted well by the steady axisymmetric wake around a rectilinear rising bubble, provided the local orientation of the wake is taken parallel to the bubble trajectory (figures 15 and 20 in Ellingsen & Risso 2001).

Risso & Ellingsen (2002) investigated a homogeneous swarm of bubbles of the same size rising in water otherwise at rest at dilute gas volume fractions ($5\times10^{-3}\leq\alpha\leq10^{-2}$). Concerning the bubbles, dual optical probe (DOP) measurements showed that their positions were randomly distributed (no clustering) and that their fluctuating velocity remained controlled by the path oscillations—bubble interactions had thus negligible effects. Using combined

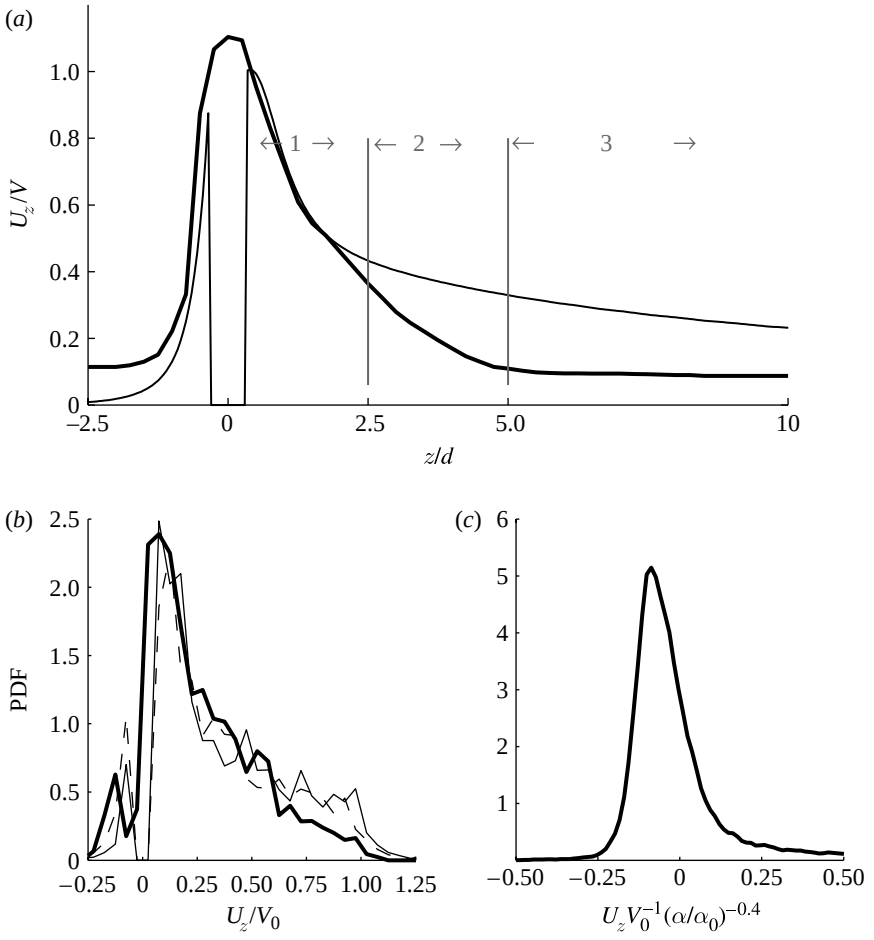

Figure 1. Liquid flow induced by rising bubbles. (*a*) Vertical velocity against the distance to the bubble for a single rising bubble and a bubble in a swarm (thin line, isolated bubble ($\alpha=0$); thick line, $\alpha=0.5\%$); (*b*) PDF of the vertical velocity in the vicinity of a bubble (thin line, $\alpha=0.64\%$; dashed line, $\alpha=1.05\%$; thick line, $\alpha=0$); (*c*) unconditioned probability density function of the vertical velocity in a swarm ($\alpha_0=10^{-2}$).

DOP and LDA measurements, the maximal liquid velocity perturbation at a given vertical distance from a test bubble was determined. Figure 1*a* compares the liquid vertical velocity perturbation induced by the bubble in the swarm for $\alpha=5\times10^{-3}$ (thick line) with the reference case of the isolated bubble (thin line). We note the existence of three regions: (i) close to the test bubble ($-2.5<z/d<2.5$), the flow is similar to that induced by a single rising bubble, (ii) further behind the bubble ($2.5\leq z/d\leq5$), interactions between individual wakes become significant and the liquid velocity decreases much faster than behind a single bubble, (iii) for larger distances ($z/d>5$), the velocity fluctuations finally reach an asymptotic state independent of the distance from the test bubble. As expected the probability density function (PDF) of the vertical liquid velocity in region (1), which is presented in figure 1*b*, is almost independent of α; its contribution to the total fluctuation is consequently proportional to α and remains small for dilute

dispersions. On the other hand, the unconditioned liquid velocity is found to scale as $V_0\alpha^{0.4}$, where V_0 is the mean rise velocity for $\alpha \to 0$. Provided the velocity is normalized by $V_0\alpha^{0.4}$, the PDF of the velocity fluctuations becomes independent of the volume fraction (figure 1*c*). It is worth noticing that this self-similar behaviour is incompatible with a linear summation of individual wakes which would provide a PDF with all centred moments proportional to α. In particular, the fact that the variance of the measured PDF increases as $\alpha^{0.8}$, i.e. with a power less than one, indicates that wake interactions are responsible for an increase of the dissipation. The validity of this self-similar behaviour has been recently confirmed experimentally for bubbles of diameters from 1.6 to 2.5 mm and volume fractions up to 14% (Riboux 2007; Riboux *et al.* 2007; Roig 2007).

Experimental investigations in high Reynolds number dilute bubbly flows have provided evidence of strong wake attenuation due to multi-body interactions. They also suggest that wakes play a major role in the dynamics of the liquid fluctuations, while the flow field generated close to each bubble is secondary. Risso & Legendre (2003) and Riboux *et al.* (2007) tested this idea by performing numerical simulations of wake interactions. Each bubble is modelled by a source of momentum added in the Navier–Stokes equations that are solved on a coarse grid, the spacing of which is close to the bubble diameter. The bubbles are fixed and placed in a uniform downward flow. For a single bubble, it was found that the wake was well reproduced for $z \geq 5d$. A large number of identical bubbles were inserted in the computational domain to model the bubble swarm. The results of the simulations are in good agreement with the measurements, confirming that neither the motions of the bubbles relative to each other nor the description of the flow close to each bubble were necessary to reproduce the statistics of the liquid fluctuations. The understanding of wake interactions is thus crucial for the understanding of dispersed two-phase flow.

3. Wake attenuation in homogeneous bubble swarms

In this section, we present quantitative measurements of the wake attenuation length L in air–water bubbly flows by two different methods: (i) conditional averaging of the velocity perturbation behind a test bubble inside a swarm and (ii) analysis of the decay of the fluctuating energy behind a swarm. Both cases consider bubble diameters in the range 1.6–2.5 mm and volume fractions in the range 3×10^{-3} to 10^{-1}. As pointed out by the wake intermingling model, the relevant length scale corresponding to the strength of the wakes is d/C_d. For these experimental conditions, Riboux (2007) showed that $d/C_\mathrm{d}(\alpha)$ is a decreasing function of α but does not depend on d. In the following, the experimental results will be normalized by the value corresponding to the lowest investigated volume fraction ($d/C_{\mathrm{d}0} = 8.6$ mm for $\alpha = 3\times10^{-3}$) in order to focus on the evolution of L with α.

The first experimental configuration was described in Roig & Larue de Tournemine (2007); it consists of a homogeneous injection of bubbles in a vertical channel flow, whose turbulent intensity in the absence of the bubbles is less than 2%. The average vertical velocity perturbation conditioned by the distance to the bubble has been measured by means of a hot film anemometer (HFA). Figure 2*a* shows the mean velocity defect ΔU normalized by the mean relative velocity between the two phases

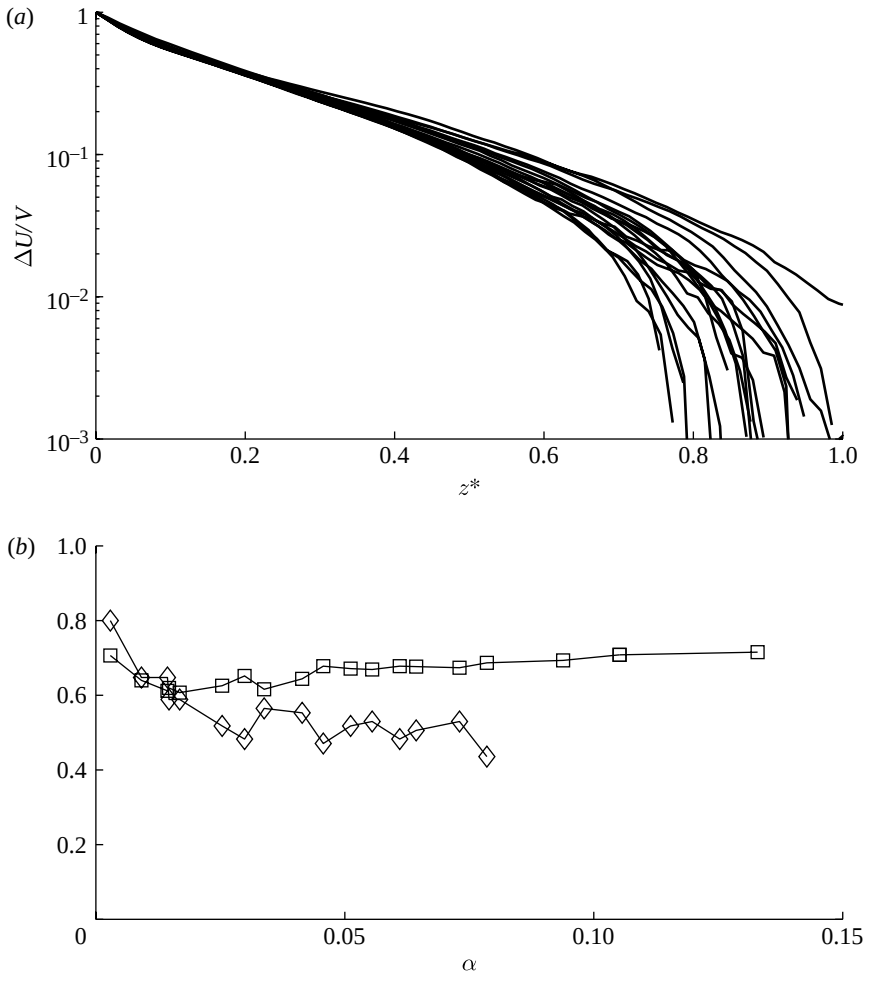

Figure 2. Wake attenuation in a homogeneous bubble swarm. (*a*) Liquid velocity perturbation against the normalized distance $z^* = zC_{\mathrm{d}0}/d$ to the test bubble for various volume fractions ($0.3\times10^{-2} \leq \alpha \leq 13\times10^{-2}$). (*b*) Attenuation length $L^* = LC_{\mathrm{d}0}/d$ and integral length scale $\Lambda^* = \Lambda C_{\mathrm{d}0}/d$ against the volume fraction (diamond, Λ^*; square, L^*).

as a function of the dimensionless distance $z^* = zC_{\mathrm{d}0}/d$ to the bubble. An exponential decay is observed up to the distance L where the velocity perturbation has already decreased by 95%, $L^* \approx 0.6$. Then, a sharp cut-off is observed and the wake totally disappears. (The curves, which are not labelled for the sake of clarity, seem to indicate that this cut-off becomes stronger as α is increased; however, the accuracy is not sufficient to conclude definitively on this point.) Surprisingly, this exponential decay is observed to be independent of α in the range investigated. A root-mean-square fitting by an exponential law has also been used to compute L for each value of α. The values of L^* are plotted in figure 2*b* together with the normalized integral length scale Λ^* of the liquid fluctuations, which was determined from temporal series of the vertical velocity by Larue de Tournemine (2001). For α larger than 10^{-2}, L^* is independent of α and close to Λ^*.

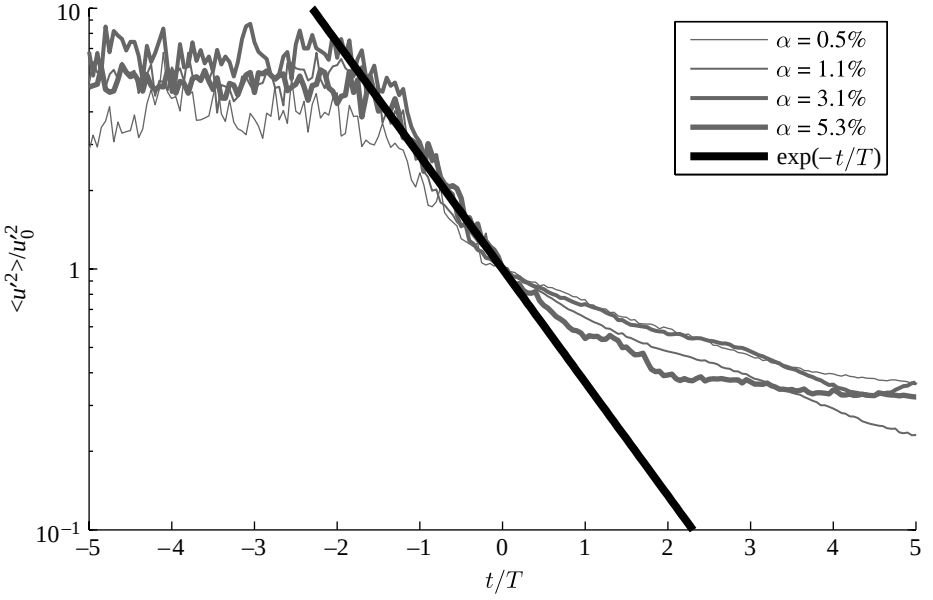

Figure 3. Evolution of the vertical velocity variance in the wake of the whole swarm as a function of time for various volume fractions.

In the second experiment, a steady homogeneous swarm of rising bubbles is first produced by continuous injection of air from the bottom of a tank. The gas injection is then suddenly interrupted so that a frontier between a two-phase mixture and a region where there is no bubble is observed to propagate upward at velocity V (for details see Riboux 2007). The liquid velocity is measured by high-speed particle image velocimetry (Hi-PIV) in a fixed vertical window located in the middle of the tank and 400 mm above the injection, where the bubbly flow no longer depends on the elevation. Figure 3 shows the temporal evolution of the variance of the velocity fluctuations $\overline{u'^2}$ as the frontier goes up over the measurement window for volume fractions between 5×10^{-3} and 5.3×10^{-2}. The first part of the signals, which shows a plateau, corresponds to measurements inside the bubble swarm where the variance is constant. After the passage of the frontier, we observe a first regime where the variance decays as $\exp(-t/T)$, followed by another regime where it decays as $\exp(-t/T_2)$ with $T^2 > T$. Provided the variance has been normalized by its value $u_0'^2$ at a given instant, say $t=0$, the results match for all α and give $T=0.2$ s. We have no way to compare T with L. However, the main point is that the attenuation of the wake of the whole bubble swarm is exponential and independent of α.

The present results show that multi-body interactions are responsible for exponential decay of the wakes. The characteristic length of attenuation L scales as d/C_{d0} as it can be expected from the wake intermingling mechanism. However, this length has been observed to be independent of α in the range $10^{-2} \leq \alpha \leq 10^{-1}$, whereas the average distance between the bubbles l_{b} varies from $3.7d$ to $1.7d$. It is worth noting that the wake attenuation saturates, while the overall energy of the liquid fluctuations induced by the bubble motions still increases with α. The physical mechanism responsible for this saturation is still not understood.

It probably remains unchanged for larger volume fractions as long as the spatial distribution of the bubble remains homogeneous, and also for other bubble diameters provided the Reynolds number is sufficiently large for the wakes to remain predominant. However, it can be influenced by the properties of the ambient flow since the saturation is observed to occur from a slightly smaller volume fraction in the case of bubbles rising in a fluid at rest ($\alpha = 5 \times 10^{-3}$) than in the case of bubbles rising in a turbulent channel flow ($\alpha = 10^{-2}$).

4. Wake of a sphere in an ambient turbulent flow

It is known that the wake of a fixed sphere immersed in a uniform incident turbulent flow is attenuated compared with that of a sphere in a uniform laminar flow (Wu & Faeth 1994*a*,*b*). The scope of this section is to check whether the mechanism of wake attenuation caused by shear-induced turbulence is the same as that caused by multi-body interactions. To answer this question it is useful to investigate the wake of a body in an ambient turbulence, whose length scale Λ and intensity $\sqrt{\overline{u'^2}}/V$ are close to those of fluctuations induced by body motions. For a large Reynolds number ($100 \leq Re \leq 1000$) and moderate volume fractions ($10^{-2} \leq \alpha \leq 10^{-1}$), $\sqrt{\overline{u'^2}}/V$ is quite large, typically 0.2–0.4, and Λ is of the same order as d.

A few works have studied the wake of a sphere in an incident turbulent flow for Reynolds numbers in this range. Wu & Faeth (1994*a*,*b*) experimentally investigated rather low turbulence intensities ($0.01 \leq \sqrt{\overline{u'^2}}/V \leq 0.07$) and large turbulent scales ($10 \leq \Lambda/d \leq 60$). Bagchi & Balachandar (2004) made direct numerical simulations for adequate turbulent intensities ($0.1 \leq \sqrt{\overline{u'^2}} \leq 0.25$) but for even larger turbulent scales ($50 \leq \Lambda/d \leq 300$). Legendre *et al.* (2006) performed large eddy simulations for $\sqrt{\overline{u'^2}} = 0.04$ and $\Lambda/d = 8$. All of them observed that the velocity defect ΔU decreases as z^{-1} in the region just behind the sphere and its closed wake. Legendre *et al.* (2006) also found that ΔU decreases as z^{-2} in a second part of the wake where it becomes smaller than the incident fluctuation $\sqrt{\overline{u'^2}}$. However, none of these studies considered a turbulence with properties similar to those of dispersed two-phase flows, i.e. with a fluctuating velocity at the scale of the sphere of the same order of the velocity defect in the near wake. We have thus decided to carry out a new experimental investigation specially devoted to this problem.

A 2 cm diameter sphere is placed on the centreline of a vertical square water channel of width $b = 0.22$ m. The Reynolds number Re based on the sphere diameter is varied from 100 to 1000, the channel Reynolds number being 10 times larger. This range of Re covers contrasted regimes for a sphere in a laminar uniform flow from steady to turbulent wakes, with vortex shedding starting around $Re = 270$. The incident flow was previously characterized by LDA in the absence of the sphere—the mean flow is uniform and the turbulence is almost homogeneous and isotropic; the integral length scale Λ is approximately $3d$ for all Reynolds numbers, a value that is common for a turbulent channel flow. The vertical $\sqrt{\overline{u'^2_z}}/V$ and horizontal $\sqrt{\overline{u'^2_x}}/V$ turbulent intensities decrease from 0.26

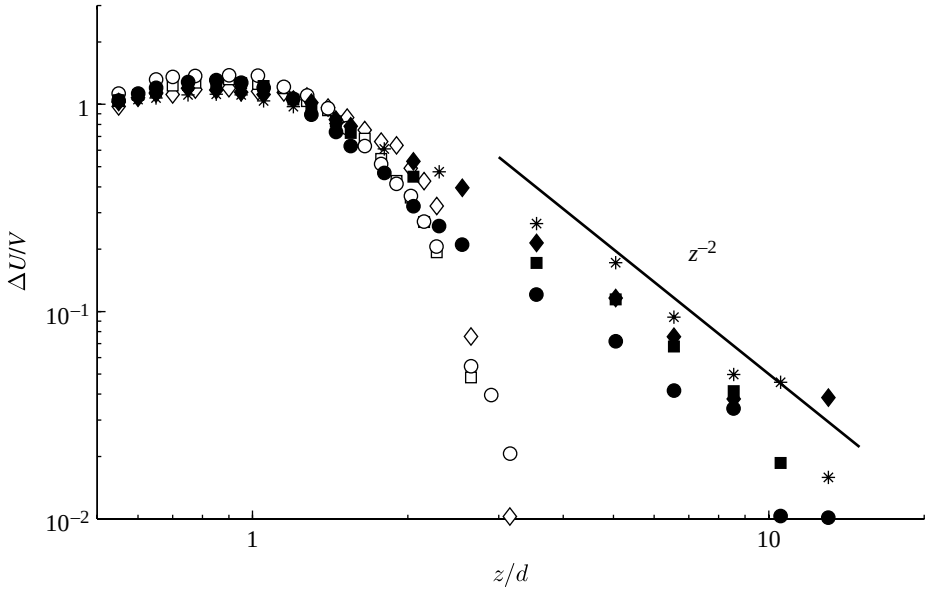

Figure 4. Velocity defect against the distance from a sphere in either an incident turbulence (Re=asterisk 110, filled diamond 230, filled square 670, filled circle 1090) or in a random array of spheres (Re=open diamond 235, open square 700, open circle 1120).

to 0.12 when the Reynolds number increases from 100 to 400 and then remain constant for larger Re. The velocity defect $\Delta U/V$ on the axis is plotted against the vertical distance to the sphere z/d in figure 4. In the near wake ($z/d \leq 1.5$), the only visible effect of the incident turbulence is to slightly shorten the length of the recirculation region, which varies a little with the Reynolds number up to $Re=670$, where it becomes independent of Re. However, the main feature is that the wake decays as z^{-2} just downstream from the recirculating zone for all investigated Reynolds numbers. The reason is that the intensity of the external imposed turbulence at the scale of the wake is already comparable to the velocity defect from the beginning of the open wake.

Even if the turbulence properties were chosen as close as possible to those of the bubble-induced fluctuations, the wake decay was observed to follow a z^{-2} power law instead of the exponential law observed in bubbly flows. Shear-induced turbulence thus seems less efficient to attenuate wakes than multi-body interactions, suggesting that the involved mechanisms are different. However, one could say that there are many differences between freely rising bubbles and fixed rigid spheres, which weaken this conclusion. We shall propose a more relevant comparison by considering a random array of fixed spheres in §5.

5. Wake of a sphere in a random array of spheres

We use the same experimental set-up as for the study of the isolated sphere in an incident turbulence, but insert 200 identical spheres in order to obtain a volume fraction $\alpha=2.16\times10^{-2}$. The 2 cm spheres are randomly distributed over the channel. They are maintained by 97 steel rods that have a negligible influence on

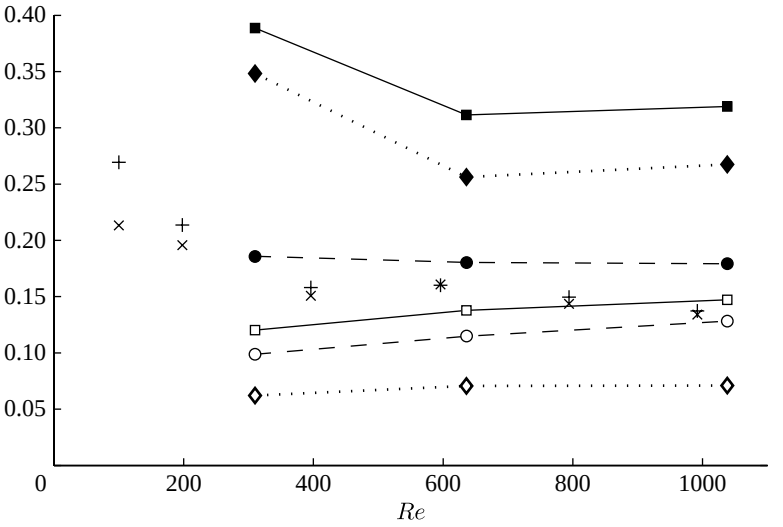

Figure 5. Various contributions to the fluctuations as a function of the Reynolds number. Turbulence intensity in the channel in the absence of the spheres, $\times$ $\sqrt{\overline{u_x'^2}}/V$ and $+$ $\sqrt{\overline{u_z'^2}}/V$. Intensity of the fluctuations in the random array of spheres: total fluctuations, open squares $\sqrt{\langle u_x^2\rangle}/V$, filled squares $\sqrt{\langle u_z^2\rangle}/V$; spatial contribution, open diamonds $\sqrt{\langle \overline{u_x}^2\rangle}/V$, filled diamonds $\sqrt{\langle \overline{u_z}^2\rangle}/V$; temporal contribution, open circle $\sqrt{\langle u_x'^2\rangle}/V$, filled circle $\sqrt{\langle u_z'^2\rangle}/V$.

the flow since their diameter is less than 2 mm and their total volume is less than one-tenth that of the spheres. Reynolds numbers in the range 235–1120 were investigated.

Single-point LDA velocity measurements were performed to determine the integral length scales $\mathbf{\Lambda}$ and velocity variances $\langle u'^2\rangle$. Note that here the variance is obtained by spatial averaging of the square of the fluctuation $u'(\boldsymbol{x}, t)$, which is the difference between the local instantaneous velocity $u(\boldsymbol{x}, t)$ and the local time-averaged velocity $\bar{u}(\boldsymbol{x})$, in order to provide a quantity relevant for the statistical description of the turbulence inside the network. The values of Λ increase from $2d$ to $3d$ as Re increases from 235 to 1120. The vertical and horizontal turbulent intensities, $\sqrt{\langle u_z'^2\rangle}/V$ and $\sqrt{\langle u_x'^2\rangle}/V$, are plotted against Re in figure 5. The fluctuating energy in the network flow is close to that in the channel flow and evolves similarly with Re. Both the turbulence integral length scale and energy are thus apparently not drastically changed by the presence of the network, but a significant anisotropy is now observed, $\sqrt{\langle u_z'^2\rangle}$ being larger than $\sqrt{\langle u_x'^2\rangle}$.

In figure 4, the velocity defect behind a sphere belonging to the network is plotted for Re=235, 700 and 1120. For all Reynolds numbers, a much stronger attenuation than that for the isolated sphere takes place. We cannot formally conclude whether it is an exponential decay due to the narrow range of z available; it is however undoubtedly of a different nature unlike the decay behind the isolated sphere (which follows a z^{-2} law) and looks like the decay observed in bubbly flows. Note that the velocity defect presented in figure 4 corresponds to a unique sphere; consequently accurate quantitative determination of the attenuation length is not possible. However, the same qualitative

behaviour has been observed for several other spheres and the present result does, therefore, not correspond to a singular event. This work is still currently in progress and ensemble averages are not available at the present time. A crude estimate of the attenuation length can nevertheless be obtained from figure 4: $L \approx 2.5d$. Estimating the drag coefficient from the Schiller and Nauman correlation (Clift *et al.* 1978) for a sphere in a laminar flow, one finds that d/C_d ranges from $1.3d$ to $2.4d$ for $235 \leq Re \leq 1120$, which is close to the measured value of L.

The results obtained for a sphere in a network suggest that the mechanism of wake attenuation is the same for fixed solid spheres and moving bubbles, which can be expected from the fact that large-scale simulations of the flow in a network of fixed momentum sources are capable of reproducing the statistics of the fluctuations measured in a swarm of rising bubbles (Risso & Legendre 2003; Riboux *et al.* 2007). Moreover, the present results also confirm that wake attenuations in homogeneous shear-induced turbulence are different from those caused by multi-body interactions. In §6 we discuss the reasons for this difference.

6. Perspectives

Why are multi-body interactions so efficient at enhancing wake spreading? A way to address this question is to find out the properties of the fluctuations induced by moving bodies, which make them different from shear-induced turbulence. Let us consider first a particular realization of an isotropic and homogeneous turbulent flow. The velocity fluctuations are due to many eddies of different sizes which are created, die, move and exchange energy, their dynamics being described by the classic Kolmogorov cascade. All the statistical moments of the velocity fluctuation can be determined by considering a single instant and averaging in a given spatial direction over a length sufficiently large compared with the integral length scale Λ. It can also be determined by time averaging at a given point. The flow is said to be ergodic in both time and space. Now, let us consider a single realization of a homogeneous swarm of bubbles rising at velocity V. Again, spatial averaging converges towards ensemble averaging, provided the spatial domain contains a sufficiently large number of sub-domains of size larger than Λ to constitute a representative sample of all possible spatial bubble distributions. Time averaging at a given point leads to the same result because all possible spatial bubble distributions will be encountered at the considered point as the bubbles rise. In the laboratory frame, a homogeneous bubble swarm thus also appears to be ergodic in both space and time. Two differences from classic turbulence have however been noted. First, the fluctuations are not isotropic in two respects: (i) the variance of the vertical fluctuations is larger than that of the horizontal ones and (ii) the PDF of vertical fluctuations is asymmetric—large upward fluctuations being more probable than large downward ones (figure 1*c*). Point (ii) constitutes a major difference since classic turbulence is unlikely to be able to maintain vertical homogeneity when upside-down symmetry is broken, non-zero dissymmetry coefficients being usually associated with a turbulence gradient (Risso & Fabre 1997). A second difference is that the spectral signature of bubble-induced turbulence differs from the classic $-5/3$ power law (Lance & Bataille 1991),

indicating that the dynamics of the fluctuating eddies is different. The bubble-induced turbulence is commonly considered as a turbulence in which energy is injected at an intermediate scale close to the bubble diameter instead of being supplied by the largest scales of the flow. The difference in nature between classic turbulence and bubble-induced turbulence is, however, more profound.

Let us consider now the homogeneous swarm of rising bubbles in a frame that moves at velocity V. If we neglect the motion of the bubbles relative to each other, we are left with a uniform mean flow V across a fixed array of bubbles. Although spatial averaging still converges towards ensemble averaging, time averaging no longer does so. For instance, it is clear that the time-averaged velocity $\overline{U}(\boldsymbol{x})$ at a point $\boldsymbol{x}$ located just downstream of a bubble is lower than V, whereas it is larger beside a bubble. A simple Galilean change of frame is thus sufficient to break down time ergodicity. Denoting time averaging by an overbar, we decompose the instantaneous velocity $u(\boldsymbol{x}, t) = U(\boldsymbol{x}, t) - V$ at each point $\boldsymbol{x}$ in time-averaged and fluctuating contributions,

$$u(\boldsymbol{x}, t) = \overline{u}(\boldsymbol{x}) + u'(\boldsymbol{x}, t). \tag{6.1}$$

Denoting the spatial averaging by brackets, the total variance of the velocity can be decomposed into two contributions

$$\langle u^2 \rangle = \langle \overline{u}^2 \rangle + \langle u'^2 \rangle. \tag{6.2}$$

The first contribution $\langle \overline{u}^2 \rangle$ is related to the spatial variations of the time-averaged velocity, the random character of them being due to the random character of the spatial distribution of the bubbles. Imagine a situation in which both the perturbation generated by each body is steady and the multi-body interactions do not destabilize the flow; in the frame that moves at velocity V the flow is laminar and steady, however $\langle \overline{u}^2 \rangle$ is different from zero. The spatial contribution $\langle \overline{u}^2 \rangle$ has, therefore, nothing to do with turbulence. On the other hand, the second contribution $\langle u'^2 \rangle$ is related to temporal fluctuations and measures the turbulence intensity in large Reynolds number flows. (Note that if we considered the motions of the bubbles relative to each other, a third contribution should be taken into account.)

Since the spatial and temporal contributions correspond to different physical mechanisms, an important step towards the understanding of high Reynolds number-dispersed two-phase flows lies in the decomposition of the fluctuations in their spatial and temporal contributions. Currently, there is a lack of suitable diagnostic tools that can be appropriately applied to decompose the temporal and spatial contributions to the flow from a swarm of moving bodies. However, this is easy to do in an array of fixed bodies. Figure 5 shows the evolutions against the Reynolds number of the total intensity of the fluctuations $\sqrt{\langle u^2 \rangle}/V$ as well as those of the temporal $\sqrt{\langle u'^2 \rangle}/V$ and the spatial $\sqrt{\langle \overline{u}^2 \rangle}/V$ contributions. The spatial contribution is larger than the temporal one in the vertical direction, whereas it is the opposite in the horizontal direction. This is made possible by the strong predominance of the vertical fluctuations in the spatial contribution, $\sqrt{\langle \overline{u_z}^2 \rangle} \approx 4\sqrt{\langle \overline{u_x}^2 \rangle}$, which is probably related to the quasi-parallel structure of the wakes.

Comparing the magnitude of the temporal and spatial contributions is nevertheless insufficient since there is no reason to assume that their roles in the enhancement of the wake spreading are similar. If the role of the temporal contribution can probably be analysed with classic turbulence tools, the spatial one probably requires new concepts. From the present results, it seems reasonable to think that the spatial contribution is mainly responsible for the enhancement of the wake decay since, as has already been noted in §5, the temporal contribution is of the same order as the turbulent intensity measured in the channel in the absence of the network of spheres.

In the future, an extensive investigation of the properties of the velocity fluctuations within a network of spheres and comparisons with those of homogeneous bubbly flows should lead to a better understanding of the mechanisms of momentum diffusion in dispersed two-phase flows.

The authors would like to thank the FERMaT research group in Toulouse for supporting this project.

References

Bagchi, P. & Balachandar, S. 2004 Response of the wake of an isolated particle to an isotropic turbulent flow. *J. Fluid Mech.* **518**, 95–123. (doi:10.1017/S0022112004000989)

Calfish, R. E. & Luke, H. C. 1985 Variance in the sedimentation speed of a suspension. *Phys. Fluids* **28**, 759–760. (doi:10.1063/1.865095)

Cartellier, A. & Rivière, R. 2001 Bubble-induced agitation and microstructure in uniform bubbly flows at small to moderate particle Reynolds numbers. *Phys. Fluids* **13**, 2165–2181. (doi:10.1063/1.1381562)

Clift, R., Grace, J. R. & Weber, M. E. 1978 *Bubbles, drops and particles*, ch. 5, p. 111. Mineola, NY: Dover Publications, Inc.

Eames, I., Roig, V., Hunt, J. C. R. & Belcher, S. E. 2004 Vorticity annihilation and inviscid blocking in multibody flows. In *Flow and transport processes with complex obstructions*. NATO Science Series. Amsterdam, The Netherlands: Springer.

Ellingsen, K. & Risso, F. 2001 On the rise of an ellipsoidal bubble in water: oscillatory paths and liquid induced velocity. *J. Fluid Mech.* **440**, 235–268. (doi:10.1017/S0022112001004761)

Hunt, J. C. R. & Eames, I. 2002 The disappearance of laminar and turbulent wakes in complex flows. *J. Fluid Mech.* **457**, 111–132. (doi:10.1017/S0022112001007236)

Koch, D. L. 1993 Hydrodynamic diffusion in dilute sedimenting suspensions at moderate Reynolds numbers. *Phys. Fluids A* **5**, 1141–1155. (doi:10.1063/1.858600)

Lance, M. & Bataille, J. 1991 Turbulence in the liquid phase of a uniform bubbly air–water flow. *J. Fluid Mech.* **222**, 95–118. (doi:10.1017/S0022112091001015)

Larue de Tournemine, A. 2001 Etude expérimentale de l'effet du taux de vide en écoulement diphasique à bulles. PhD thesis, Institut National Polytechnique, Toulouse.

Legendre, D., Merle, A. & Magnaudet, J. 2006 Wake of a spherical bubble or a solid sphere set fixed in a turbulent environment. *Phys. Fluids* **18**, 048 102. (doi:10.1063/1.2191885)

Parthasarathy, R. N. & Faeth, G. M. 1990 Turbulence modulation in homogeneous dilute particle-laden flows. *J. Fluid Mech.* **220**, 485–514. (doi:10.1017/S0022112090003354)

Riboux, G. 2007 Hydrodynamique d'un essaim de bulles en ascension. PhD thesis, Institut National Polytechnique, Toulouse.

Riboux, G., Risso, F. & Legendre, D. 2007 Liquid fluctuations generated by large-Reynolds-number rising bubbles. In *Proc. Int. Conf. of Fluid Multiphase Flow, Leipzig, Germany, 9–13 July 2007*.

Risso, F. & Ellingsen, K. 2002 Velocity fluctuations in a homogeneous dilute dispersion of high-Reynolds-number rising bubbles. *J. Fluid Mech.* **453**, 395–410. (doi:10.1017/S0022112001006930)

Risso, F. & Fabre, J. 1997 Diffusive turbulence in a confined jet experiment. *J. Fluid Mech.* **337**, 233–261. (doi:10.1017/S0022112097004965)

Risso, F. & Legendre, D. 2003 Velocity fluctuations induced by high-Reynolds-number rising bubbles: experiments and numerical simulations. *ERCOFTAC Bull.* **March**, 41–45.

Roig, V. 2007 Hydrodynamique des écoulements diphasiques dispersés, transfert de masse et mélange en écoulements à bulles. HDR thesis, Institut National Polytechnique, Toulouse.

Roig, V. & Larue de Tournemine, A. 2007 Measurement of interstitial velocity of homogeneous bubble flows at low to moderate void fraction. *J. Fluid Mech.* **572**, 87–110. (doi:10.1017/S0022112006003600)

White, B. L. & Nepf, H. M. 2003 Scalar transport in random cylinder arrays at moderate Reynolds number. *J. Fluid Mech.* **487**, 43–79. (doi:10.1017/S0022112003004579)

Wu, J. S. & Faeth, G. M. 1994*a* Sphere wakes at moderate Reynolds numbers in a turbulent environment. *AIAA J.* **32**, 535–541.

Wu, J. S. & Faeth, G. M. 1994*b* Effect of ambiant turbulence intensity on sphere wakes at intermediate Reynolds numbers. *AIAA J.* **33**, 171–173.